International Journal of Earth, Energy and Environmental Sciences
ISSN: 2517-942X
Vol:9, No:4, 2015

Ab initio Study of Co_2ZrGe and Co_2NbB Full Heusler Compounds

Abada Ahmed, Hiadsi Said, Ouahrani Tarik, Amrani Bouhalouane, Amara Kadda

***Abstract*—**Using the first-principles full-potential linearized augmented plane wave plus local orbital (FP-LAPW+lo) method based on density functional theory (DFT), we have investigated the electronic structure and magnetism of full Heusler alloys Co_2ZrGe and Co_2NbB. These compounds are predicted to be half-metallic ferromagnets (HMFs) with a total magnetic moment of 2.000 μ_B per formula unit, well consistent with the Slater-Pauling rule. Calculations show that both the alloys have an indirect band gaps, in the minority-spin channel of density of states (DOS), with values of 0.58 eV and 0.47 eV for Co_2ZrGe and Co_2NbB, respectively. Analysis of the DOS and magnetic moments indicates that their magnetism is mainly related to the *d-d* hybridization between the Co and Zr (or Nb) atoms. The half-metallicity is found to be relatively robust against volume changes. In addition, an atom inside molecule AIM formalism and an electron localization function ELF were also adopted to study the bonding properties of these compounds, building a bridge between their electronic and bonding behavior.
As they have a good crystallographic compatibility with the lattice of semiconductors used industrially and negative calculated cohesive energies with considerable absolute values these two alloys could be promising magnetic materials in the spintronic field.

***Keywords*—**Electronic properties, full Heusler alloys, half-metallic ferromagnets, magnetic properties.

I. Introduction

THANKS to the opportunity that offer the *ab initio* calculations, many hypothetical compounds with exciting properties have been offered theoretically in an effort to satisfy the endless demand of new functional materials. Of particular, interest are half-metals (HM), i.e., compounds for which only the one spin direction presents a gap at the Fermi level (E_F) while the other has a metallic character leading to 100% spin-polarization. HM materials offer a number of potential applications in spintronic devices [1]-[4]. The behavior of HMFs was firstly predicted by de Groot et al [5]. Later, half-metallic ferromagnetism has been observed in many materials, such as Heusler compounds [6]-[11]. Up to recently, the research has been practically performed on many Co_2- based full-Heusler alloys Co_2YZ where Y is a transition metal and Z is a main group element. These alloys present one appealing aspect and they are prospective candidates for application in the spintronic devices. This is due to their high Curie temperature beyond room temperature and the simple fabrication process. For example, the measured Curie temperatures are 985 K for Co_2MnSi, 905 K for Co_2MnGe [12], and 1100 K for Co_2FeSi [13].

The HMFs act as a spin filter that provides current with a high degree of spin polarization. Materials with high spin polarization can be used for tunnel magnetoresistance (TMR) and giant magnetoresistance (GMR) [14], [15]. A recent ferromagnetic shape memory alloys have been discovered in some Heusler alloys [16]-[18]. Despite the strong demand motivated by the above applications, accurate calculation of electronic and magnetic properties on this family of material remains challenging.

To our knowledge, there are a relatively fewer investigations till now for Co_2- based Heusler compounds with 4*d* transition metal elements. Recently, some magnetic properties of the ferromagnetic Heusler alloys Co_2YSn (Y= Ti, Zr, Nb) have been measured by [19]. Afterwards, the magnetism of Co_2ZrZ (Z= Al, Sn) had been investigated theoretically and by experiments [20], [21]. Later, [22] predicted that Co_2ZrSi is a HM ferromagnet using *ab initio* calculations. More recently, [23] studied the electronic structure and half-metallicity of Co_2ZrGe using first-principles calculations based on pseudopotential method.

The purpose of this study is to calculate the electronic structures, magnetic and bonding properties of the Co_2ZrGe and Co_2NbB Heusler alloys, with $AlCu_2Mn$-type structure, by first-principles calculations based on the FP-LAPW+lo method and to use them to predict HMFs. Moreover, the central insight here is to understanding the role of *d* orbitals in the electronic properties and in the mechanism of ferromagnetism for both Co_2ZrGe and Co_2NbB compounds.
In this paper, we present calculations related to the structural properties. We also report band structures, DOS and the total and atomic magnetic moments. We further study the bonding properties with both AIM and ELF formalisms.

The outline of the paper is as follows. In Section II, we briefly describe the details of our calculations. After, we present the results for the electronic, magnetic and bonding properties of these compounds in Section III. Finally, we conclude our results in Section IV.

II. Computational Details

The geometry optimization and electronic structure calculations are carried out using the FP-LAPW+lo method within DFT [24] implemented in the WIEN2k package [25].

A. Abada is with the Laboratoire d'Etudes Physico- Chimiques, Université Dr Moulay Tahar Saida 20000, Algeria (corresponding author to provide phone: + 213 557 11 79 55; e-mail: ahmedabada72@yahoo.fr).
S. Hiadsi is with Département de Génie Physique, Université d'Oran des Sciences et de la Technologie Mohamed Boudiaf, Algeria.
T. Ouahrani is with Ecole Préparatoire Sciences et Techniques, Département de Physique BP 165 R.P., 13000 Tlemcen, Algeria.
B. Amrani is with Département de Physique, Université d'Oran Es-Sénia, Oran 31000, Algeria.
K. Amara is with the Laboratoire d'Etudes Physico- Chimiques, Université Dr Moulay Tahar Saida 20000, Algeria.

The generalized gradient approximation (GGA) proposed by Perdew, Burke, and Ernzerhof (GGA-PBE96) was used for the exchange-correlation functional [26]. We take full relativistic effects for core states, use the scalar approximation for the valence states, and neglect the spin-orbit coupling. We take $R_{mt}K_{max}$ equal to 8.0 where R_{mt} is the smallest of the muffin tin sphere radius and K_{max} is the largest reciprocal lattice vector used in the plane wave expansion. We make the angular momentum expansion up to l_{max} = 10 in the muffin tins spheres. The radii R_{mt} of the muffin tins are chosen to be large as possible under the condition that the spheres do not overlap and to minimizing the interstitial space. The cutoff energy, which defines the separation of valence and core states, was chosen as -6.0 Ry. At convergence the integrated difference between input and output charge densities was less than 10^{-4}. We use 3000 k points in the first Brillouin zone (BZ) (according to the Monkhorst-Pack scheme [27], 14 x 14 x 14 k-points sampling grid were used). The BZ integrations for the total energy have been carried out using 104 special k-points in the symmetry-irreducible volume of the BZ to construct the charge density in each self-consistency step.

One popular route to exploit wave functions in the study of bonding properties is to do topological analysis of electronic density based on an algorithm involving grid partition.

III. Results and Discussion

A. Structural Properties

The full Heusler compounds are ternary intermetallic alloys with the chemical formula X_2YZ, where X and Y are different transition metals and Z is a nonmagnetic *sp* element. The two full Heusler alloys Co_2ZrGe and Co_2NbB are predicted to crystallize in $L2_1$ structure (space group Fm-3m no.225), with $AlCu_2Mn$ as the prototype. In this structure, the lattice consists of four interpenetrating face-centered-cubic (fcc) sublattices. The unit cell is a fcc lattice with four atoms as X at A (0,0,0) and C (1/2,1/2,1/2) sites, Y at B (1/4,1/4,1/4) and Z at D (3/4,3/4,3/4) sites in Wyckoff coordinates. In this arrangement, each X atom has four Y and four Z atoms as nearest neighbors while each Y and Z atom is surrounded by eight X atoms.

The $AlCu_2Mn$-type structure is predicted to be more favorable than the $CuHg_2Ti$-type structure for the two compounds Co_2ZrGe and Co_2NbB because Zr and Nb atoms are less electronegative than Co as zirconium and niobium have fewer valence electrons than the cobalt atoms. For 3*d* transition metals, it is found those elements with more valence electrons are favorable to occupy the A and the C sites and with fewer ones occupy the B sites [9]. In this study, we can also verify this trend for 4*d* elements Zr and Nb. Indeed, we have calculated the total energy as function of the cell volume per formula unit for the ferromagnetic (FM) states of both $AlCu_2Mn$ and $CuHg_2Ti$ types of full-Heusler alloys Co_2ZrGe and Co_2NbB. It can be seen, from Fig. 1 (a) and Fig. 1 (b), that for both compounds, the equilibrium energy of the $CuHg_2Ti$-type is higher than that of $AlCu_2Mn$-type, which indicate that the latter structure is energetically more stable. As a result, Co atoms occupy preferentially the A and the C sites. The Zr and Nb atoms prefer occupying the B sites.

We then calculate the total energy as function of the cell volume per formula unit for the FM and paramagnetic (PM) states of the $AlCu_2Mn$-type structure of the considered Heusler alloys. From Fig. 1 (c) and Fig. 1 (d), we note that for these systems, the FM phases have lower energies than the PM phases. As seen from these figures, the energy difference between the FM and PM states at their corresponding equilibrium lattice increases with the atomic number of the Z atoms. This means that a large Z atom is needed in stabilizing the FM state. We can also see that this energy difference increases slightly with increasing cell volume (i.e., with increasing lattice constant). The values of the energy difference between FM and PM states were listed in Table I. We have gathered also in this table the calculated equilibrium lattice constants for the FM phase, the bulk modulus *B* and its pressure derivative *B*', that are determined by fitting the total energy as a function of volume to the Murnaghan equation of state [28].

The equilibrium lattice constants for Co_2ZrGe and Co_2NbB are 6.08 Å and 5.67 Å, respectively. It is noted that the obtained lattice constant for Co_2ZrGe is in agreement with preceding theoretical calculation [23]. It is clear that the calculated lattice constant of Co_2NbB is smaller than that of Co_2ZrGe due to the smaller atomic radius of B than that of Ge. The bulk modulus decreases according to the following sequence (see Table I): $B(Co_2ZrGe) < B(Co_2NbB)$, i.e. in reverse order of lattice parameters. This is consistent with the relationship between *B* and the lattice constant *a* (*B* is proportional to V_0^{-1} [29] where V_0 is the primitive cell volume). In the absence of experimental data for the materials under study, no comment can be assigned to the accuracy of our results.

We have reported also in Table I the cohesive energy E_{Coh} which is defined as the equilibrium total energy of the alloy minus the sum of the total energies of the pure atomic constituents of these compounds. The cohesive energy reflects the strength of the force that links atoms together in the solid state.

The calculations show that the cohesive energies are -23.01 and -25.97 eV/f.u. for Co_2ZrGe and Co_2NbB, respectively. We note that the calculated values of cohesive energy are negative and the absolute values are considerable. Thus, these values guarantee the physical stability of the two compounds against decomposition in the $L2_1$ structure. To the best of our knowledge, no experimental or theoretical data are available for comparison.

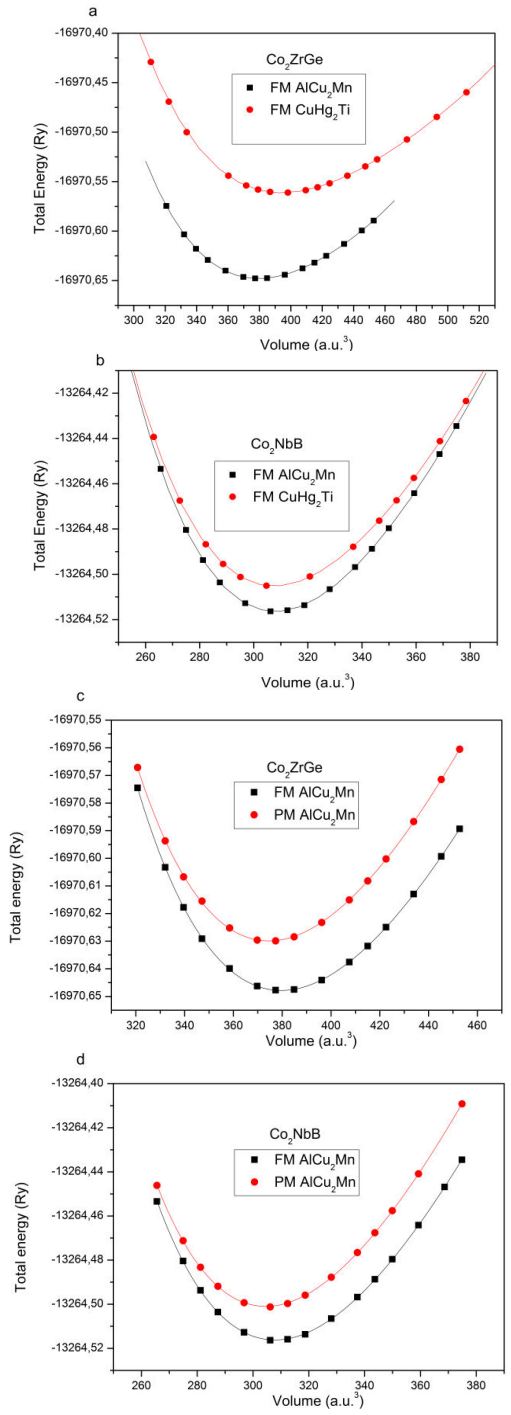

Fig. 1 (a) Total energy as a function of the cell volume per formula unit for Co_2ZrGe in the $AlCu_2Mn$ and $CuHg_2Ti$-type structures in the FM states. (b) The same curve for Co_2NbB. (c) The volume optimization for Co_2ZrGe in the PM and FM states with the $AlCu_2Mn$ -type structure. (d) The same curve for Co_2NbB.

TABLE I
THE CALCULATED EQUILIBRIUM LATTICE CONSTANT (a), BULK MODULUS (B), ITS PRESSURE DERIVATIVE (B'), ENERGY DIFFERENCE ($\Delta E = E_{FM} - E_{PM}$) BETWEEN PARAMAGNETIC AND FERROMAGNETIC STATES, COHESIVE ENERGY (E_{Coh}), MINORITY-SPIN GAP (G_{Min}) AND HM GAP (G_{HM}) FOR Co_2ZrGe AND Co_2NbB

Symbol	Co_2ZrGe	Co_2NbB
a (Å)	6.08 6.06 [23]	5.67
B(GPa)	168.78	237.13
B'	4.74	4.80
ΔE(meV)	-243.49	-206.42
E_{Coh} (eV/f.u)	-23.01	-25.97
G_{Min} (eV)	0.58 0.43 [23]	0.47
G_{HM} (eV)	0.31	0.28

B. Electronic Properties

Furthermore, we have presented the spin-polarized band structures of FM Co_2ZrGe and Co_2NbB at equilibrium lattice constants along their high-symmetry directions in the Brillouin zone, as shown in Fig. 2. For these entitled compounds, the majority-spin channel is found metallic whereas in the minority-spin channel there is an energy gap G_{Min}. Therefore, we can forecast that these systems could be HMFs. The band structure plot shows that the valence band extends up to around -11 eV and -10 eV below the Fermi level E_F for Co_2ZrGe and Co_2NbB, respectively. According to Fig. 2, in the minority-spin channel (the dashed dot lines), the indirect band gaps along the Γ-X symmetry for Co_2ZrGe and Co_2NbB are 0.58 eV and 0.47 eV, respectively. The obtained value of the gap for Co_2ZrGe is larger than that found by preceding calculation [23]. There is no experimental data for the comparison.

The Fermi level for these compounds lies nearly in the middle of the gap. It locates at 0.31 eV and at 0.28 eV above the highest minority-spin valence bands of Co_2ZrGe and Co_2NbB, respectively. Hence, there is a HM gap (spin-flip gap) G_{HM}, i.e., the minimum energy required to flip a minority-spin electron from the valence band maximum to the majority-spin Fermi level. The minority-spin bands gaps G_{Min} and the HM gaps G_{HM} are also presented in Table I. The values of the G_{HM} are 0.31 eV and 0.28 eV for Co_2ZrGe and Co_2NbB, respectively. The non-zero spin-flip gaps suggest that these alloys are true HMFs. We can note that these values are relatively large thus they are more stable in practical applications than the ones with a small G_{HM}.

According to the studies, relaying on the group theory, of [7], [8], the hybridization in $L2_1$ structure occurs not only between the Co 3*d* orbitals and its first nearest neighbours Zr (or Nb) 4*d* orbitals or Ge (or B) *sp* states but also between the second nearest neighbour Co-Co 3*d* orbitals. Moreover, in case of full-Heusler alloys the origin of energy gap in minority spin channel is also governed by the interaction between the two Co atoms and between Zr (or Nb) and *sp* atoms [30]. The interaction between Co and its second nearest neighbour Co atom causes non-bonding states (t_{1u} and e_u) in the minority spin channel near E_F. We consider the hybridization of the Co-Co orbitals with the Zr (or Nb) 4*d* orbitals with the same

transforming representation. The three t_{1u} states are below the Fermi level and they are occupied while the two empty e_u are just above E_F [7], [8]. The absence of hybridization between e_u and t_{1u} states of Co and Zr (or Nb) atoms results a splitting. The energy gap in minority spin states is traced back to this e_u - t_{1u} splitting.

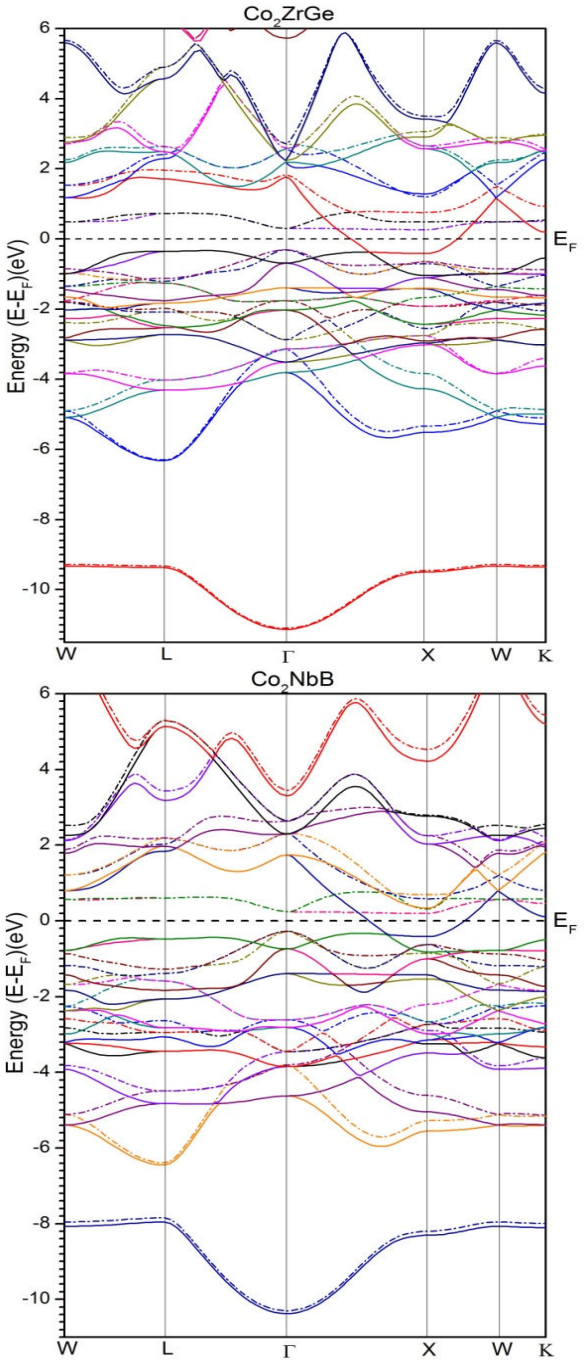

Fig. 2 Spin-polarized band structures along the principal high-symmetry directions in the Brillouin zone of Co_2ZrGe and Co_2NbB at their predicted equilibrium lattice constants. The dashed dot lines correspond to minority-spin channel and the solid lines correspond to majority-spin channel

According to Fig. 2, in the minority-spin and majority-spin channels, it is outstanding that the energy region between -6 eV and -3 eV (or - 4 eV) is originates mainly of the three energy bands of *p* electrons of the Ge (or B) atoms. The *s* band is very low in energy and well isolated from other bands. It is located around -9 eV (or -8 eV) and extended to -11 eV (or -10 eV) for Co_2ZrGe (or Co_2NbB). The energy bands between - 3 eV and 5.5 eV for Co_2ZrGe and between - 4 eV and 4.5 eV for Co_2NbB are attributed to the strong hybridizations between the *d* states of transition metals which create the bonding and antibonding states. The energy bands below E_F in minority-spin channel from -3 eV (or -4 eV) to -1 eV for Co2ZrGe (or Co2NbB) are mostly made up of five bonding bands ($2\times e_g$ and $3\times t_{2g}$) plus three t_{1u} non-bonding Co states located at around -1 eV (or -1.3 eV). The bands above E_F are relative to two e_u non-bonding Co states (around 0.5 eV) and five antibonding bands ($2\times e_g$ and $3\times t_{2g}$) extended from 1.5 eV to 5.5 eV for Co_2ZrGe and from 1 eV to 4.5 eV for Co_2NbB. For Co_2ZrGe (or Co_2NbB), the upper edge of the t_{1u} state is located at 0.31 eV (or 0.28 eV) below the Fermi level, and the lowest edge of the e_u state is at 0.27 eV (or 0.19 eV) above the Fermi level so that the band gap is 0.58 eV (or 0.47 eV) and the Fermi level locates almost at the middle in the gap between e_u and t_{1u} states of Co atoms.

Now, we discuss our results pertaining to the electronic properties of the investigated compounds, at their equilibrium lattice constants, via the DOS. Calculated spin-polarized total and partial densities of states (DOSs) are shown in Fig. 3 and Fig. 4. It is seen that there is an energy gap around E_F in the minority DOS indicating semiconducting character, while in the majority spin there is a DOS peak, which leads to 100% spin polarization at the Fermi level in these alloys. This implies that Co_2ZrGe and Co_2NbB are HM compounds. From these figures, it is clear that the energy region between -6 eV and -3 eV (or - 4 eV) is relative to *p* bands of the Ge (or B) atoms. The *s* band is very low in energy (around -9 eV and -8 eV for Ge and B atoms, respectively) and also is well separated from other bands. The band structure of *s* and *p* states is almost identical for both directions. The Ge (or B) atoms provide *s* and *p* states to be hybridized with *d* electrons of Co and Zr (or Nb) atoms and determine the degree of occupation of the *p*-*d* orbitals. As seen from Fig. 3 and Fig. 4, the partial DOSs of Co 3*d* orbitals, in the two materials, show the same behavior. We can also notice that the DOS around and below E_F is mostly associated with the Co 3*d* states which confirm that the bonding states mostly exist at the higher valence transition metal Co atom. While, the partial DOSs of Zr (or Nb) 4*d* orbitals lies mainly above the Fermi level, i.e., the unoccupied antibonding bands mainly exist at the lower valence transition metal Zr (or Nb) atom [6].

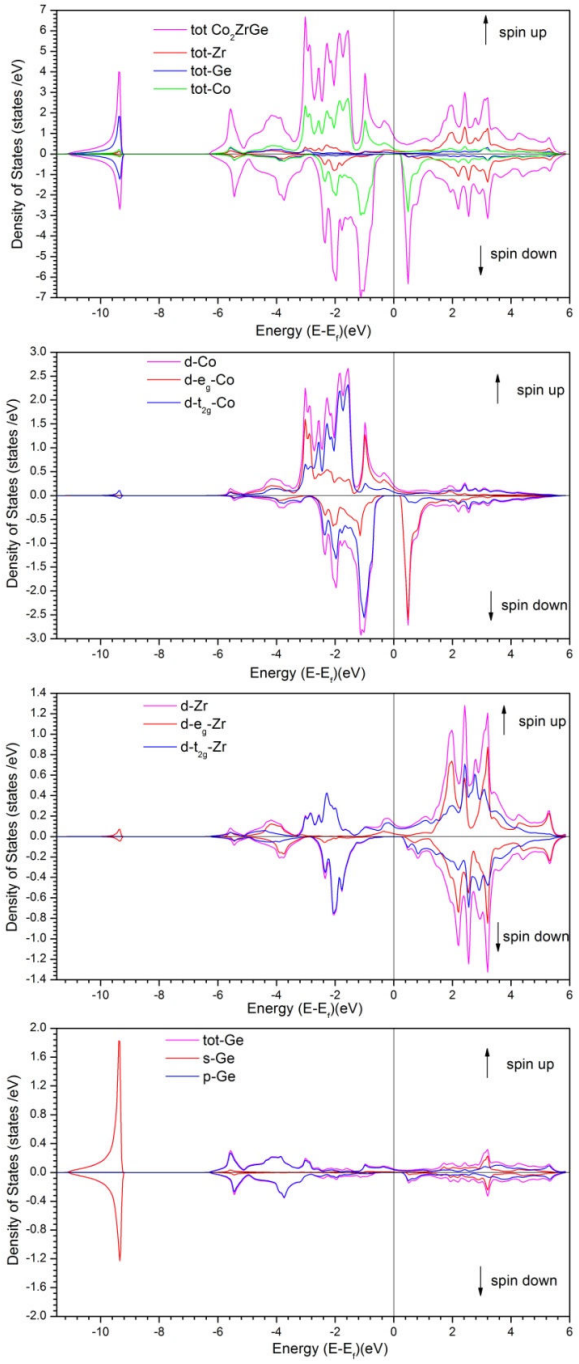

Fig. 3 Spin-dependent total and partial DOSs of Co_2ZrGe projected on the three atoms at its predicted equilibrium lattice constant. In each row, the panel is the calculation with volume optimization. The upper or lower part of every panel is the majority-spin DOS or the minority-spin DOS. The energy zero is set at the Fermi level. (For interpretation of the references to color in this figure legend, the reader is referred to the web version of this article)

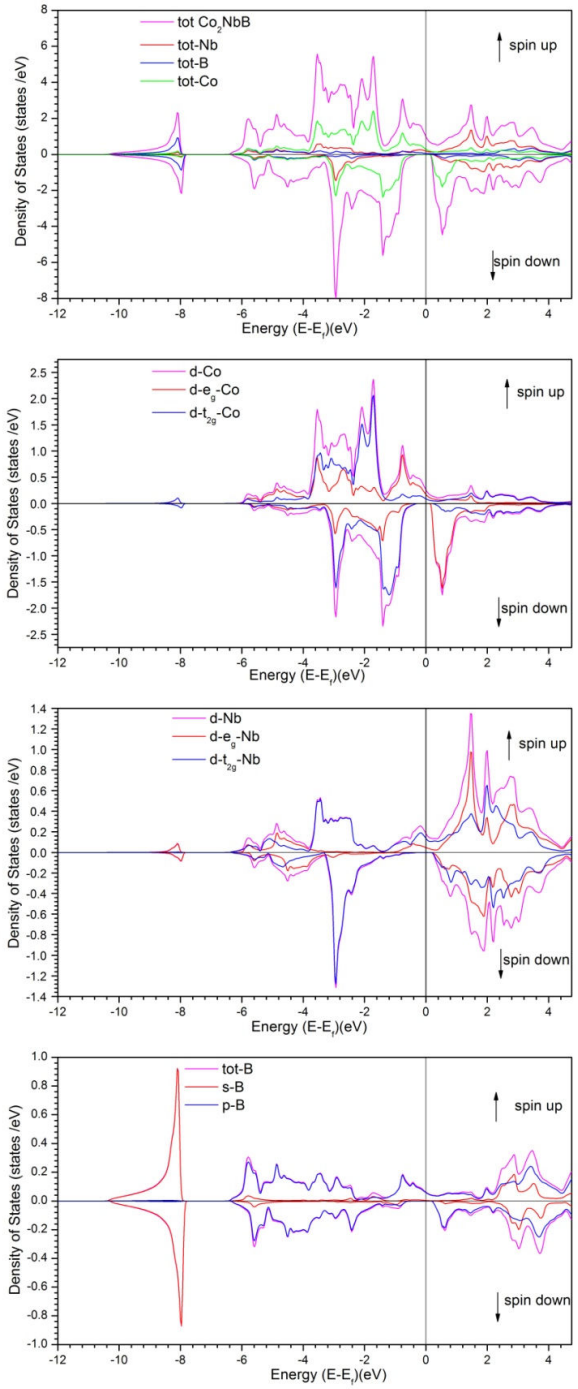

Fig. 4 Spin-dependent total and partial DOSs of Co_2NbB projected on the three atoms at its predicted equilibrium lattice constant. (For interpretation of the references to color in this figure legend, the reader is referred to the web version of this article)

From partial DOSs, it is seen that the gap is larger for the Zr (or Nb) and *sp* atoms than for the Co one. This difference can be traced back to the spin down t_{1u} and e_u states around the gap which are localized at the Co and do not couple with any of the Zr (or Nb) *d* orbitals. Therefore, the peaks below and

just above the E_F are due to the t_{1u} and the e_u states, respectively. This also explains why the gaps are relatively small for Co_2ZrGe and Co_2NbB compounds.

C. Magnetic Properties

The calculated total magnetic moment per unit cell at their equilibrium lattice constants in the compounds is exactly 2.000 μ_B. An integer value of magnetic moment is a typical characteristic of HMFs [3], [5], [31]. Table II shows the calculated total, atom-resolved magnetic moments and contribution of interstitial regions for Co_2ZrGe and Co_2NbB.

TABLE II
THE CALCULATED MAGNETIC MOMENTS IN THE UNIT OF μ_B, THE CO ATOM MOMENT (M_{Co}), Y ATOM MOMENT (M_Y) (Y = Zr, Nb), Z ATOM MOMENT (M_Z) (Z = Ge, B), INTERSTITIAL MOMENT (M_{int}), AND THE UNIT CELL TOTAL MAGNETIC MOMENT (M_{tot}) FOR Co_2ZrGe AND Co_2NbB

Symbol	Co_2ZrGe	Co_2NbB
M_{Co}	1.07216 1.02 [23]	1.00321
M_Y	-0.07004 -0.08 [23]	-0.02043
M_Z	0.02961 0.04 [23]	0.06066
M_{int}	-0.10381	-0.04661
M_{tot}	2.00007 2.00 [23]	2.00004

Heusler alloys are considered to be ideal local moment systems. In the two alloys, the magnetic moment is mainly localized on the Co atoms. Indeed, these atoms contribute a large and positive magnetic moment (1 μ_B). This is attributed to the large exchange splitting between the majority and minority spin states of Co atoms. Therefore, in case of Co_2ZrGe and Co_2NbB most of the share of magnetic moment arises from Co atoms, where two Co atoms together have a total magnetic moment about 2 μ_B. We have also noticed that the partial moment of Zr (or Nb) atoms is slightly antiferromagnetically spin polarized to Co and *sp* moments of the systems. It emerges from the hybridization with the transition metals and is caused by the overlap of the electron wave functions. As shown in Table II, the *sp* atoms carry a negligible magnetic moment which does not contribute much to the overall moment. The small moments found at the *sp* sites are mainly due to polarization of these atoms by the surroundings, magnetically active atoms [9]. A small negative amount of magnetic moment is found in the interstitial region too. It is noted that the calculated partial magnetic moments of Co_2ZrGe present a tiny discrepancy compared to the values of [23] which is mainly due to the difference of the calculated minority-spin band gaps. This leads to a decrease of the Co moment in [23] which was compensated by increasing the partial spin moments of Zr (with absolute values) and Ge atoms in comparison to our values.

The calculated total magnetic moment satisfies the rule of 24 [7] which is the analogue of the Slater-Pauling behavior in the full-Heusler alloys. In this rule, the relation for the total magnetic moment M_{tot} per formula unit and the total number Z_{tot} of valence electrons in the unit cell is:

$$M_{tot} = (Z_{tot} - 24)\ \mu_B.$$

For Co_2ZrGe and Co_2NbB, Z_{tot} = 26, 18 from the two Co atoms, 4 from Zr (5 from Nb) and 4 from Ge (3 from B). The magnetic moment is exactly 2 μ_B per unit cell in agreement with our *ab initio* results.

Since the lattice constant of an epitaxially grown film depends on the lattice constant of the substrate and deviate from the equilibrium value, it is important to study the robustness of the half-metallicity with respect to variation of the lattice constants. For this purpose, the calculations have been performed for the lattice parameters between 5.40 Å and 6.06 Å for Co_2NbB and between 5.75 Å and 6.45 Å for Co_2ZrGe. Fig. 5 shows the total magnetic moment per formula unit for the full-Heusler alloys Co_2ZrGe and Co_2NbB as a function of the lattice constant. The total magnetic moments remain integer with the compression and expansion of lattice constants with respective equilibrium lattices over a relatively wide range. Indeed, it is seen in Fig. 5 that the half-metallicity character is appeared above the lattice constant values of 5.46 Å and 5.82 Å for Co_2NbB and Co_2ZrGe, respectively. It is maintained up to 6.06 Å and 6.45 Å for the two compounds. Therefore, the half-metallicity can be robust against volume changes when the lattice constants are changed by -3.7% to 6.9% and -4.3% to 6.1% relative to the equilibrium lattice constants for Co_2NbB and Co_2ZrGe, respectively. It is worth to indicate that our calculations show that the half-metallicity for Co_2ZrGe is more robust against lattice constant changes than that of [23] (5.99-6.47 Å). This discrepancy can be traced back to the difference between the FP-LAPW+lo and the pseudopotential methods.

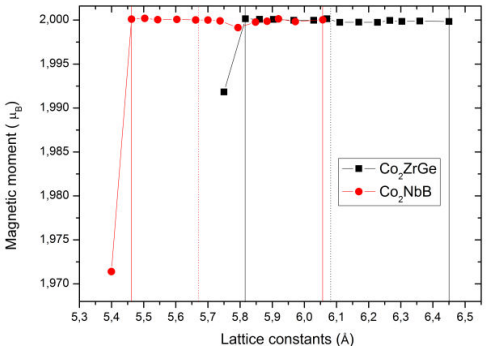

Fig. 5 Total magnetic moment (units of μ_B) as a function of the lattice constants for Co_2ZrGe and Co_2NbB. The black and red vertical dotted lines indicate the equilibrium lattice constants and the black and red vertical solid lines show the range of half-metallicity of Co_2ZrGe and Co_2NbB, respectively. (For interpretation of the references to color in this figure legend, the reader is referred to the web version of this article)

As the equilibrium lattice constants of Co_2ZrGe and Co_2NbB compounds (6.08–5.67 Å) are close to that of zinc blende semiconductors such as InAs (6.058 Å), CdSe (6.077 Å), ZnTe (6.088 Å), GaSb (6.096 Å), AlSb (6.135 Å) and GaAs (5.655 Å), AlAs (5.661 Å), ZnSe (5.667 Å) [32], respectively, it is suggested to experimentally realize these

HM Heusler alloys in the form of thin films on appropriate substrates and to use them as new candidates for applications in spintronic field.

D.Bonding Properties

The topological elements of the $\nabla\rho$ (ρ being the electronic density and ∇ the gradient vector) field are the carriers of a wealthy chemically relevant information, and the critical points ($\nabla\rho = 0$), for instance, are the generators of the molecular graph [33]. The theory has been extremely successful in recovering chemical concepts from both experimental [34] and theoretical [33] densities and it is now well developed in both molecular [35] and condensed matter [36] realms. A systematic study of the complete topology of the electron density in a Co_2ZrGe and Co_2NbB Heusler alloys seems to be lacking. Accordingly, our focus will be addressed more towards an investigation of the local bonding properties, within two sophisticated approaches, atom in molecule theory (AIM) [37] and electron localization function (ELF) [38]. The simplest model of a metal is constituted by a periodic array of positively charged ions embedded in a uniform homogeneous electron gas. For this model the attractors of the density gradient field are located on the nuclei of the ion whereas the jellium background gives rise to an infinite number of non-hyperbolic critical points. To undertake such investigation, an *ab initio* calculation will be performed with a state-of-the-art electronic structure method, namely the FP-LAPW methodology.

Due to the difference of the electronegativity between Zr and Nb atoms, both compounds show some difference in their topology and charge transfer between atoms (see Fig. 6). As it is known from Pauling concept, the metallic bond is basically a partial covalent bond. We have exploited the ratio of the net charges of an atom in a material and the charges of its nominal oxidation state to calculate the charges transfer and the ionicity degree. We have found respectively that the degree of the covalent character in the Co_2ZrGe and Co_2NbB compounds have 89 and 79 percent. In the Co_2NbB compound, the net charges of Co, Nb and B atoms are -1.7536986963e, +1.1003001352e and +0.51534922343e (e is the fundamental charge), respectively, whereas in the Co_2ZrGe compound, the net charges of Co, Zr and Ge atoms are -0.4624989919e, +1.2566370614e and +0.38978545226e, respectively.

This prominent chemical bonding features from AIM point of view can be also showed by the calculated Electron Localized Function (ELF) [38] iso-surface plots, as displayed in Fig. 7. The dimensionless ELF magnitude ranges from 0 to 1 with ELF = 1/2 corresponding to the free electron gas distribution, ELF = 0 points to no localization, when ELF = 1, it corresponds to perfect electron localization.

Further evidence of the complete delocalization comes from the representation in Fig. 7 of the 1D ELF plots of the two Heusler.

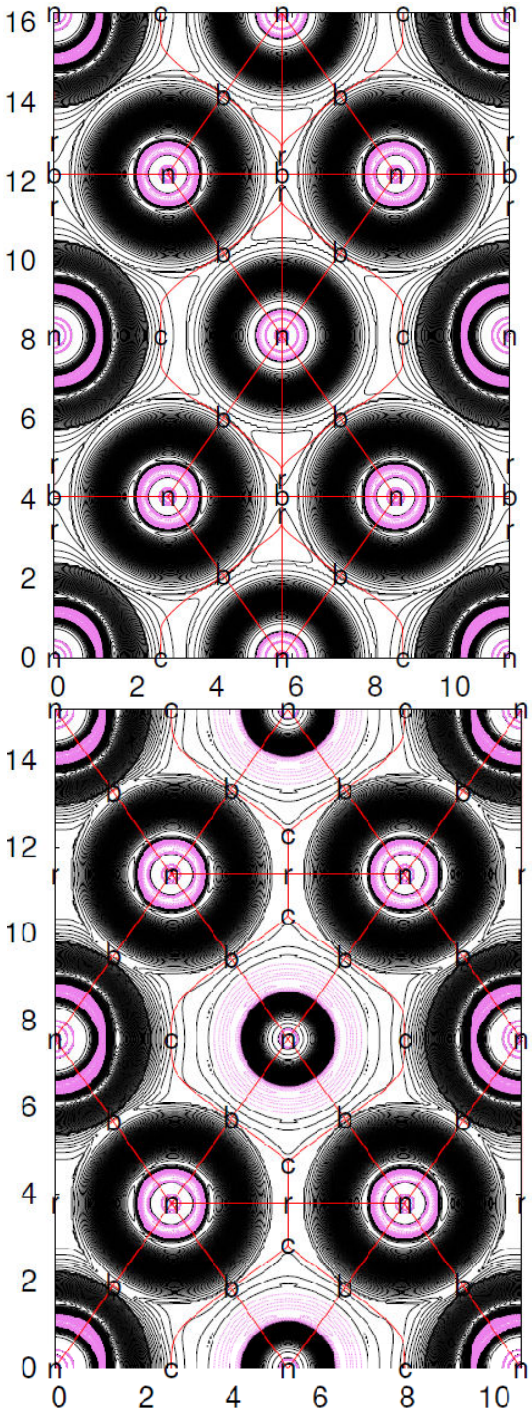

Fig. 6 In red lines, trajectories traced out by electron density gradient vector field (in electron/bohr^3) of (top side) Co_2ZrGe and (bottom side) Co_2NbB at the optimal FP-LAPW geometry. The set of trajectories that terminates at each bond critical points (b) defines an interatomic surface. The set of trajectories that originate at the ring critical (r) points define the perimeter of the interatomic surface. The gradient paths associated with the negative eigenvalues at the (n) point terminate at this CP and define the zero-flux surfaces that partition the crystal into unique fragments (the atomic basins)

The electron localization is created from an unsteadiness of the electronic charge due to the dipole moment. In order to investigate further the electron distribution in a semi quantitative manner, we perform the integrations of atomic properties within each basin bounded by the critical points (CP's). For all atoms found in the two compounds, an ELF maximum was found for each atomic shell. Close to the nucleus, the (3,-3) attractor shell has an ELF value of approximately 1 (see Fig. 7). The successive ELF maxima mark the atomic shells. There are two possibilities for the ELF shape of the valence (last) shell. If the atom has only *s* electrons in the valence shell, then the localization for the valence shell grows fast to a high value (almost 1.0) and reaches the maximal localization at infinity. As a signature of metallic behavior, the ELF attractors form a connected network. The charge density is relatively flat, which facilitates the ability of electronic conduction.

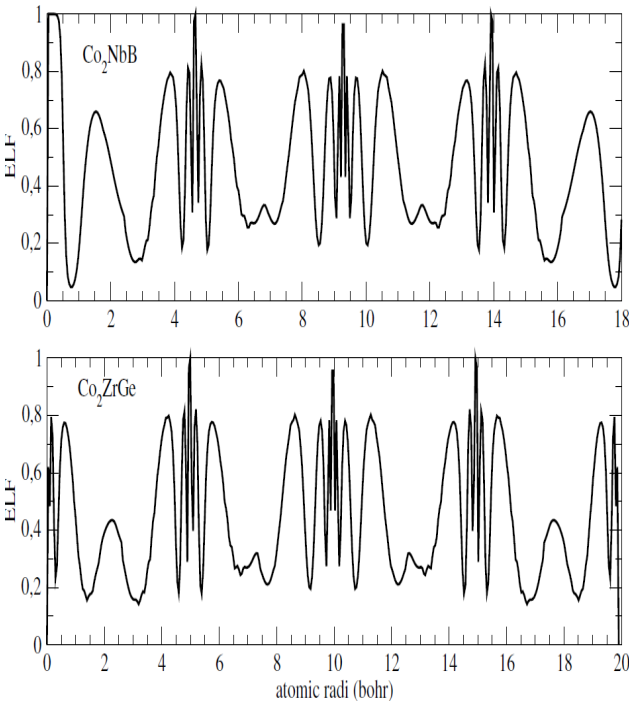

Fig. 7 ELF plots as function of atomic radii of the Co_2NbB and Co_2ZrGe compounds

IV. Conclusion

In summary, we have used the FP-LAPW+lo method based on DFT within the GGA to investigate the electronic structure and magnetism of the full-Heusler alloys Co_2ZrGe and Co_2NbB. We found that they prefer to crystallize in the $AlCu_2Mn$-type structure rather than the $CuHg_2Ti$-type structure. We have performed the total energy calculations to find the stable magnetic configurations and the optimized lattice constants. The calculated equilibrium lattice constants for Co_2ZrGe and Co_2NbB are 6.08 Å and 5.67 Å, respectively, which match well with many semiconductor substrates. We found that the Co_2ZrGe and Co_2NbB compounds are predicted to be true HMFs with indirect band gaps of 0.58 eV and 0.47 eV, respectively, in the minority-spin channel while the majority-spin is found metallic which leads to 100% spin polarization at the Fermi level in these alloys. From the electronic band structure calculations, we found that the HM gaps of these compounds are 0.31 eV and 0.28 eV for Co_2ZrGe and Co_2NbB, respectively. The present calculation also allows us to reveal the basic mechanism for the formation of the gap in the minority-spin states. It shows that the hybridization of the Co-Co orbitals with the Zr (or Nb) *d* orbitals is essential for the formation of the gap at E_F. The gap is traced back to the splitting e_u - t_{1u}.

The calculated total magnetic moment of Co_2ZrGe and Co_2NbB is an integer number of 2.000 μ_B per formula unit which satisfies the Slater-Pauling rule. This moment is located mostly at the Co atoms.

Another interesting point addressed in this work was the study of the bonding properties with both AIM and ELF formalisms. The compounds show a trend towards non-shared interactions and a softening of the curvatures of the electron density in the bonding regions. Valence electron is labile and metallic.

These compounds are in good crystallographic compatibility with the lattice of semiconductors used industrially. In addition, the estimated values of cohesive energy are negative and the absolute values are considerable which guarantee the physical stability of the two compounds against decomposition in the $L2_1$ structure. The half-metallicity of these systems is preserved when the lattice constants are changed by -3.7% to 6.9% and -4.3% to 6.1% relative to the equilibrium lattice constants for Co_2NbB and Co_2ZrGe, respectively. The robustness in half-metallic character is advantageous to experimentally realize these HM Heusler alloys in the form of thin films on appropriate substrates. Therefore, the above outcomes indicate that Co_2ZrGe and Co_2NbB could be promising magnetic materials for applications in spintronic field. Finally, we hope that the present work will bring a support to other studies.

References

[1] A. Prinz, *Science* 282 (1998)1660.
[2] S. A. Wolf, D. D. Awschalom, R. A. Buhrman, J. M. Daughton, S. von Molnar, M. L. Roukes, A. Y. Chtchelkanova, and D. M. Treger, *Science* 294 (2001) 1488.
[3] W. E. Pickett and J. S. Moodera, *Physics Today* 54 (2001) 39.
[4] J. de Boeck, W. van Roy, J. Das, V. Motsnyi, Z. Liu, L. Lagae,H. Boeve, K. Dessein, and G. Borghs, *Semicond.Sci. Technol*. 17 (2002) 342.
[5] R. A. de Groot, F. M. Mueller, P. G. van Engen, and K. H. J.Buschow, *Phys. Rev. Lett*. 50 (1983) 2024.
[6] I. Galanakis, P.H. Dederichs, and N. Papanikolaou, *Phys. Rev. B* 66 (2002) 134428.
[7] I. Galanakis, P.H. Dederichs, and N. Papanikolaou, *Phys. Rev. B* 66 (2002) 174429.
[8] I. Galanakis, Ph. Mavropoulos, and P.H. Dederichs, *J. Phys. D: Appl. Phys*. 39 (2006) 765.
[9] H.C. Kandpal, G. H. Fecher, and C. Felser, *J. Phys. D: Appl. Phys*. 40 (2007) 1507.
[10] K. Özdoğan, I. Galanakis, E. Şaşıoğlu, and B. Aktaş, *Solid State Commun*. 492 (2007) 142.
[11] F. Ahmadian and A. Salary, *Intermetallics*. 46 (2014) 243.
[12] M. Kawakami, Y. Kasamatsu, and H. Ido, *J. Magn. Magn. Mater*. 70 (1987) 265.

[13] S. Wurmehl, G.H. Fecher, H.C. Kandpal, V. Ksenofontov, C. Felser, H.-J. Lin, and J. Morais, *Phys. Rev. B* 72 (2005) 184434.
[14] G. Schmidt, D. Ferrand, L. W. Molenkamp, A. T. Filip, and B. J. van Wees, *Phys. Rev. B* 62 (2000) R4790.
[15] K. Yakushi, K. Saito, K. Takanashi, Y. K. Takahashi, and K. Hondo, *Appl. Phys. Lett*. 88, (2006) 082501.
[16] S.R. Barman and A. Chakrabarti, *Phys. Rev. B* 77 (2008) 176401.
[17] H. Luo, G. Liu, F. Meng, S. Li, W. Zhu, G. Wu, X. Zhu, and C. Jiang, *Physica B: Condens. Matter* 405 (2010) 3092.
[18] H. Luo, G. Liu, Z. Feng, Y. Li, L. Ma, G. Wu, X. Zhu, C. Jiang, and H. Xu, *J. Magn. Magn. Mater*. 321 (2009) 4063.
[19] A. Yamasaki, S. Imada, R. Arai, H. Utsunomiya, S. Suga, T. Muro, Y. Saitoh, T. Kanomata, and S. Ishida, *Phys. Rev. B* 65 (2002) 104410.
[20] T. Kanomata, T. Sasaki, H. Nishihara, H. Yoshida, T. Kaneko, S. Hane, T. Goto, N. Takeishi, and S. Ishida, *J. Alloys. Compd*. 393 (2005) 26.
[21] W. Zhang, Z. Qian, Y. Sui, Y. Liu, W. Su, M. Zhang, Z. Liu, G. Liu, and G. Wu, *J. Magn. Magn. Mater*. 299 (2006) 255.
[22] J. Y. Jiu and J. I. Lee, *J. Korean. Phys. Soc*. 51 (2007) 155.
[23] S. Li, Y. Liu, Z. Ren, X. Zhang, and G. Liu, *J. Korean. Phys. Soc*. 65 (2014) 1059.
[24] P. Hohenberg and W. Kohn, *Phys. Rev*. 136 (1964) B864; W. Kohn and L. J. Sham, *Phys. Rev*. 140 (1965) A1133.
[25] P. Blaha, K. Schwarz, G.K.H. Madsen, D. Kvasnicka, and J. Luitz, *WIEN2k: An Augmented Plane Wave + Local Orbitals Program for Calculating Crystal Properties*, Karlheinz Schwarz, Techn. Universitat Wien, Wien, Austria, 2001, ISBN: 3-9501031-1-2.
[26] J. P. Perdew, K. Burke, and M. Ernzerhof, *Phys. Rev. Lett*. 77 (1996) 3865.
[27] H. J. Monkhorst and J. D. Pack, *Phys. Rev. B* 13 (1976) 5188.
[28] F. D. Murnaghan, *Proc. Natl. Acad. Sci.* U.S.A. 30 (1944) 244.
[29] M.L. Cohen, *Phys. Rev. B* 32 (1985) 7988.
[30] S.C. Lee, T.D. Lee, P. Blaha, and K. Schwarz, *J. Appl. Phys*. 97 (2005) 10C307.
[31] H.C. Kandpal, V. Ksenofontov, M. Wojcik, R. Seshadri, and C. Felser, *J. Phys. D: Appl. Phys*. 40 (2007) 1587.
[32] W. Martienssen and H. Warlimont, *Springer Handbook of Condensed Matter and Materials Data* (Springer, Berlin, Heidelberg 2005), ISBN: 3-540-44376-2.
[33] R. F. W. Bader and H. Essen, *J. Chem. Phys*. 80 (1984) 1943.
[34] T. S. Koritsanszky and P. Coppens, *Chem. Rev*. 101 (2001) 1583.
[35] R. F. W. Bader, T. T. Nguyen-Dang, and Y. Tal, *Rep. Prog. Phys*. 44 (1981) 893.
[36] A. Martin Pendas, A. Costales, and V. Luana, *Phys. Rev. B* 55 (1997) 4275.
[37] R. F. W. Bader, *Atoms in Molecules: A Quantum Theory* (Oxford: Oxford University Press, 1990).
[38] A. D. Becke and K. E. Edgecombe, *J. Chem. Phys*. 92 (1990) 5397.

Ahmed Abada is currently working toward the Ph.D. degree in the University of Sciences and Technology, Mohamed Boudiaf, Oran, Algeria. In November 1999, he joined the University Dr Tahar Moulay of Saida, Algeria, where he is currently a member in the Laboratory of Physical-Chemical Studies. His research interests include magnetism and half-metallic materials.